

## Identification and characterization of *Caenorhabditis elegans* $\gamma$ -tubulin in dividing cells and differentiated tissues

Yves Bobinnec\*, Makoto Fukuda and Eisuke Nishida

Department of Cell and Developmental Biology, Graduate School of Biostudies, Kyoto University, Sakyo-ku, Kyoto 606-8502, Japan

\*Author for correspondence (e-mail: bobinnec@nishidaCentris.biophys.kyoto-u.ac.jp)

Accepted 28 August; published on WWW 17 October 2000

### SUMMARY

$\gamma$ -Tubulin is an essential component of the microtubule-nucleation machinery and therefore plays a crucial role during mitosis. To gain further insights into the function of this protein in the events that take place during embryogenesis and differentiation, we carried out detailed studies on  $\gamma$ -tubulin during all the developmental stages of *Caenorhabditis elegans*. We identified the  $\gamma$ -tubulin gene from this organism and analyzed the localization of the protein by both immunofluorescence and GFP reporter construct. We show that  $\gamma$ -tubulin association with the centrosome is highly dynamic in mitotic cells, being massively recruited at prophase and released at anelophase. This accumulation in mitotic centrosomes is dramatic during the first embryonic divisions. We provide

the first description of the morphological changes at the centrosome level during the orientation of the mitotic spindle and the flattening of the posterior aster. Loss of function of the  $\gamma$ -tubulin gene by RNAi induces a strong polyploidization of mitotic germ cells and embryos, but does not affect meiosis and pronuclear migration. In addition, we demonstrate the prominent redistribution of  $\gamma$ -tubulin in adults at basal bodies of amphid and phasmid neurons, and at the apical membrane of polarized intestinal cells.

Key words: *Caenorhabditis elegans*, Cytoskeleton, Mitosis, Centrosome,  $\gamma$ -Tubulin

### INTRODUCTION

The main microtubule-organizing center of animal cells, the centrosome, is composed of a pair of centrioles surrounded by a fibrous pericentriolar material acting as a scaffold that concentrates both the microtubule nucleation machinery and its regulatory factors. In dividing cells, duplicated centrosomes separate at the onset of mitosis to establish the poles of the mitotic spindle. Concomitantly, the pericentriolar material will progressively develop and then disassemble as cells exit mitosis (Dictenberg et al., 1998). Microtubule nucleation depends essentially on  $\gamma$ -tubulin (Oakley et al., 1990; Joshi et al., 1992), an evolutionarily conserved and ubiquitously expressed protein. In association with several other components  $\gamma$ -tubulin forms a 25 nm diameter ring complex, the  $\gamma$ -TuRC, competent for microtubule nucleation (Zheng et al., 1995; Moritz et al., 1995).  $\gamma$ -Tubulin is also present in the cytoplasm as an inactive smaller complex (Moudjou et al., 1996; Oegema et al., 1999) that constitutes an exchangeable stock of material (Khodjakov and Rieder, 1999). Apart from this microtubule-nucleation activity,  $\gamma$ -tubulin has been shown to be a core component of the centriole (Fuller et al., 1995) where it plays a key role in daughter centriole formation (Ruiz et al., 1999).

Canonical centrosomes organized around centrioles, however, are not always found. A well-known example is the

loss of the centrioles at the onset of female meiosis that occurs in many species (Sonnenblick, 1950; Szöllösi et al., 1972; Albertson, 1984; Theurkauf and Hawley, 1992; Sluder et al., 1993). The oocyte will assemble a meiotic spindle through some mechanisms that involve microtubule nucleation around the chromatin and stabilization of the spindle poles by motors (Theurkauf and Hawley, 1992; Heald et al., 1997; Carazo-Salas et al., 1999). Acentriolar spindle assembly also occurs in a *Drosophila* established cell line (Debec et al., 1982) or in mammalian cells after disruption of the centrioles (Bobinnec et al., 1998), as well as in vitro around artificial chromosomes in the absence of centrosomes (Heald et al., 1997).

Moreover many types of differentiated cells do not display a radial, centrosome-focused array of microtubules. To comply with the acquisition of specialized functions, these cells undergo a complete reorganization of their cytoskeleton through mechanisms involving assembly and stabilization of microtubules at non-centrosomal sites (for recent reviews, see Keating and Borisy, 1999; Mogensen, 1999). During this process, some examples of redistribution of centrosomal components apart from the centrioles have been documented (Tassin et al., 1985; Mogensen and Tucker, 1987; Tucker et al., 1995; Meads and Schroer, 1995; Salas, 1999). Yet strikingly, this redistribution of centrosomal proteins to specific sites of the cell is poorly understood, and the mechanisms controlling microtubule nucleation are still unclear.

To gain some insights into the function of  $\gamma$ -tubulin during these processes, we decided to carry out an extensive study on  $\gamma$ -tubulin localization in dividing cells, as well as in differentiated tissues during all the developmental stages of an organism. The nematode *Caenorhabditis elegans* is an excellent model for this purpose, since embryonic stages are easily accessible to analysis by immunofluorescence methods, while the behavior of the protein in larval and adult stages can be followed using GFP technology.

We report first the identification of the *C. elegans*  $\gamma$ -tubulin gene. Disruption of  $\gamma$ -tubulin expression by RNA-mediated interference results in strong mitotic defects in the germline and in embryos, leading to a progressive polyploidization of the nuclei. The meiotic division itself is not affected, however, and the resulting female pronucleus is still able to migrate towards the male pronucleus. We also describe a dynamic localization of  $\gamma$ -tubulin at the mitotic centrosomes of cycling cells. In contrast most of the protein is distributed away from the centrioles in differentiated tissues. Our results support the idea that non-centrosomal microtubule-nucleating/organizing material may function as the main microtubule cytoskeleton organizing structure in some differentiated cell types.

## MATERIALS AND METHODS

### Worm strain

N2 (wild type) *C. elegans* strain was cultured on NGM plates and fed with OP50 *E. coli* strain under standard conditions (Brenner, 1974).

### Molecular analysis of *tbg-1*

*tbg-1*-specific cDNA was amplified from a cDNA library (a gift from Dr Iino, University of Tokyo) by PCR with internal primers and cloned into a pCR2.1-TOPO vector (Invitrogen, Carlsbad, USA). DNA sequencing was performed with the ABI prism BigDye Terminator kit and ABI prism sequence apparatus (Perkin-Elmer, Foster City, USA). When compared with the computer-generated sequence released by the *C. elegans* Sequencing Consortium (1998), the *tbg-1* cDNA sequence differs in two nucleotides (guanine to adenine at positions 105 and 342), owing to a one base shift in the position of the first and second intron. The *tbg-1* cDNA sequence has been submitted under GenBank Accession Number AF287259. 5' RACE analysis carried on total RNA from embryos was used, according to the manufacturer's protocol (Gibco BRL, Gaithersburg, USA), to characterize a SL2 splice leader sequence upstream of the ATG.

### $\gamma$ -Tubulin antibody production

A synthetic peptide corresponding to the C-terminal 16 amino acids of the predicted  $\gamma$ -tubulin protein from the sequence F58A4.8 (DEYKAVVQKDYLTRGL) was coupled to bovine serum albumin and injected to a rabbit. The rabbit was boosted six times and final blood was collected. Specific immunoglobulins were affinity purified by incubation with aminotoyoppearl beads (Tosoh, Japan) coupled to the immunogenic peptide. Bound immunoglobulins were recovered by standard methods.

### Western blotting experiments

To prepare protein extracts, embryos were collected by hypochlorite treatment of adults (Lewis and Fleming, 1995) and boiled for 5 minutes in Laemmli protein buffer (Laemmli, 1970). Proteins were separated on 8% SDS-PAGE, transferred to nitrocellulose membranes and processed for Western blotting in PBS (0.1%) Tween20 (5%) milk, according to standard procedures (Harlow and Lane, 1988).

Dilutions were 1:5000 for monoclonal anti- $\alpha$ -tubulin antibody, clone DM1A (Sigma chemicals, USA); 1:500 for affinity-purified polyclonal anti- $\gamma$ -tubulin antibody. For peptide competition, the antigenic peptide was added to a final concentration of 100  $\mu$ g/ml to the affinity-purified anti- $\gamma$ -tubulin antibody dilution during the incubation step.

### Immunofluorescence microscopy

Gravid N2 adults were cut in a drop of M9 buffer (Sulston and Hodgkin, 1988) containing 10 mM levamisole to release gonads, intestine and embryos. A coverslip was gently applied and the slide frozen in liquid nitrogen. The coverslip was then removed and the slide immediately immersed in cold ( $-20^{\circ}\text{C}$ ) methanol for 5 minutes. Slides were air-dried for 5 minutes. Embryos were rehydrated in PBS-BSA (1%) for 30 minutes, and incubated in PBS-BSA (3%) with primary antibodies for 1 hour. After three 10 minutes washes with PBS, secondary antibodies were applied in PBS-BSA (3%) for 1 hour. Slides were washed three times for 10 minutes with PBS and mounted in Mowiol (Calbiochem, La Jolla, USA; prepared as described by Harlow and Lane, 1988). Nuclei were stained with DAPI during the second wash. Antibodies were diluted 1:500 for DM1A, 1:2000 for affinity-purified anti- $\gamma$ -tubulin, 1:2500 for GT335 (ascite fluid), 1:3000 for MA1-071 (anti-nuclear pore complex antibody; ABR, Golden, USA). Fluorescent secondary antibodies were diluted 1:1000 for both Cy3-labeled anti-rabbit and anti-mouse antibodies (Amersham, Little Chalfont, England) and Alexa488-labeled anti-mouse antibody (Molecular Probes, Eugene, USA). Peptide competition was carried out as described above.

Microscopy was performed with a Zeiss Axiophot2 (Germany). Images were captured by a Photometrics CCD camera (Tucson, USA) and processed using Adobe Photoshop (Adobe systems, Mountain View, USA).

### Double-stranded RNA experiments

A Bluescript plasmid containing the  $\gamma$ -tubulin cDNA (clone yk80h7; the sequence lacks the first four bases) was provided by Dr Y. Kohara. The linearized vector was used as a template for in vitro transcription of sense and antisense single-stranded RNA by the Ribomax kit (Promega, Madison, USA). RNAs were purified by RNeasy kit (Qiagen) and annealed (Fire et al., 1998). Double-stranded RNA was injected into young N2 adult hermaphrodites at a concentration of 1 mg/ml. Worms were allowed to recover for 36 hours before transfer to individual plates. Alternatively, embryos and larvae were soaked in the RNA solution (1 to 3 mg/ml) for 40 hours (Timmons and Fire, 1998). Both protocols give the same phenotype. We therefore routinely used the RNA-soaking protocol for an extensive study of the phenotype. After recovery, embryos were analyzed by immunofluorescence after methanol fixation. Adults were fixed for 2 hours in Carnoy fixative (60% ethanol, 30% acetic acid, 10% chloroform), rehydrated in PBS and stained with DAPI. As a control, worms were soaked in double-stranded RNA produced from MAP kinase (*mpk-1*) cDNA (clone yk531h7, provided by Dr Kohara) or in buffer alone.

### Plasmid construction and DNA transformation

The putative *C. elegans*  $\gamma$ -tubulin gene was identified by the *C. elegans* Sequencing Consortium (1998) and termed *tbg-1* (sequence F58A4.8). 6.2 kilobases comprising all *tbg-1* coding and upstream sequences (including the two genes F58A4.9 and F58A4.10, and the 5'-most promoter sequences of the putative operon) were amplified by PCR from cosmid F58A4 and transcriptionally fused to the green fluorescent protein (GFP) coding sequence in the pPD95-75 vector, according to Cassata et al. (1998). Worms were transformed by co-injecting the resulting *tbg-1*::GFP construct (15  $\mu$ g/ml) and pRF4 vector (100  $\mu$ g/ml) as previously described (Mello and Fire, 1995). Several lines carrying extrachromosomal arrays were obtained and



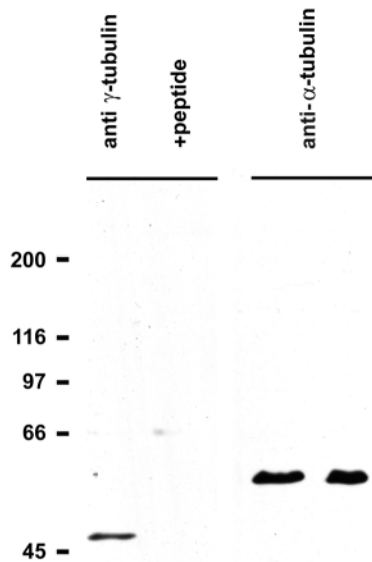


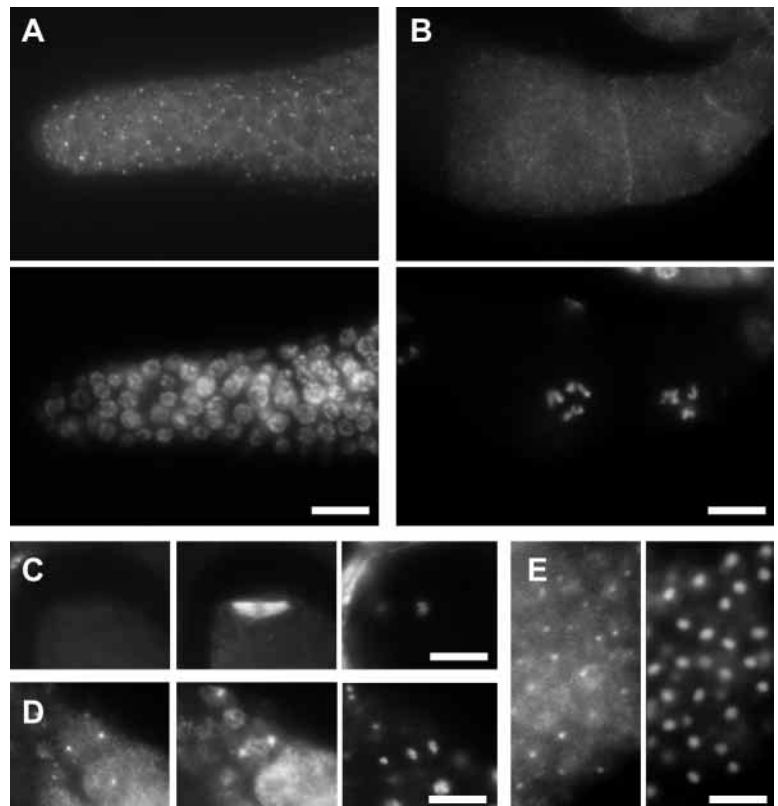
**Fig. 2.** Western blots of protein extracts from *C. elegans* embryos. Affinity-purified anti- $\gamma$ -tubulin antibody recognizes a band of 48 kDa (predicted molecular weight of 50 kDa). The immunoreactive band is eliminated by addition of the antigenic peptide during incubation (+peptide). Same membranes were reprobed with anti- $\alpha$ -tubulin antibody as a loading control.

## RESULTS

### The $\gamma$ -tubulin sequence of *C. elegans*

The recent release of the complete genome sequence of *Caenorhabditis elegans* revealed a tubulin family that comprises 16 members. The construction of a phylogenetic tree with the predicted products of these sequences together with  $\gamma$ -tubulin sequences from various organisms, shows that nine of the *C. elegans* proteins distribute as  $\alpha$ -tubulins, six as  $\beta$ -tubulins and one as  $\gamma$ -tubulin (Fig. 1A). When aligned with  $\gamma$ -tubulins from other species, this putative *C. elegans*  $\gamma$ -tubulin (also referred to TBG-1) showed many stretches of amino acids conserved

**Fig. 3.**  $\gamma$ -Tubulin distribution during female and male meiosis. Gonads from wild-type gravid hermaphrodites were dissected and processed for immunofluorescence with anti- $\gamma$ -tubulin antibody. (A-C) Female meiosis and (D-E) male meiosis. (A)  $\gamma$ -Tubulin is detected at the centrosomes of mitotic germ cells in the gonadal tip (upper panel). Lower panel shows DAPI staining of the same field. (B)  $\gamma$ -Tubulin (upper panel) displays a diffuse cytoplasmic localization in the oocytes undergoing meiosis (diplotene stage) and no centrosomal foci could be detected. Lower panel shows DAPI staining. (C) No  $\gamma$ -tubulin is detected at the acentrional poles of meiotic spindles. Left panel:  $\gamma$ -tubulin staining; middle:  $\alpha$ -tubulin; right: DAPI staining of the same spindle. These images show a metaphase II spindle. (D) Metaphase spindle during male meiosis. Left:  $\gamma$ -tubulin is detected at the poles of the centriolar spindle; middle:  $\alpha$ -tubulin; right: DAPI. (E) Mature sperm stained with anti- $\gamma$ -tubulin antibody (left) and DAPI (right). Scale bars: 10  $\mu$ m in A-D; 5  $\mu$ m in E.



in the  $\gamma$ -tubulin family (Fig. 1B), including the putative GTP-binding site. Significant divergence was found only at the C terminus end.

Sequencing of the *tbg-1* cDNA confirmed the exon structure predicted by the *C. elegans* Sequencing Consortium (minor changes are described in Materials and Methods). Furthermore, we characterized by 5' RACE analysis a splice leader sequence type 2 (SL2) upstream of the start codon, indicating that the *tbg-1* gene is part of an operon.

### Localization of $\gamma$ -tubulin during meiosis

To analyze the distribution of  $\gamma$ -tubulin in *C. elegans*, a rabbit polyclonal antiserum was raised against a synthetic peptide corresponding to the COOH-terminus of TBG-1. Western blotting analysis of a total protein extract from embryos with the affinity-purified antibody revealed a single band of a molecular weight of 48 kDa (Fig. 2). The signal was completely abolished by the addition of the immunogenic peptide during the incubation procedure, thus demonstrating the specificity of the antibody. Similarly, no signal was detected when the anti- $\gamma$ -tubulin antibody was incubated with the peptide during the immunofluorescence procedure (see Fig. 4H).

In order to determine the localization of  $\gamma$ -tubulin during female meiosis, immunofluorescence was carried out on dissected gonads from gravid wild-type hermaphrodites with the affinity-purified antibody.  $\gamma$ -Tubulin was detected at the centrosomes of mitotic germ cells localized at the distal tip of the gonad (Fig. 3A). In meiotic cells arrested at the pachytene stage in the middle of the gonad,  $\gamma$ -tubulin staining of the centrosomes was more difficult to visualize. In oocytes arrested in diakinesis of prophase I in the proximal gonad we could only

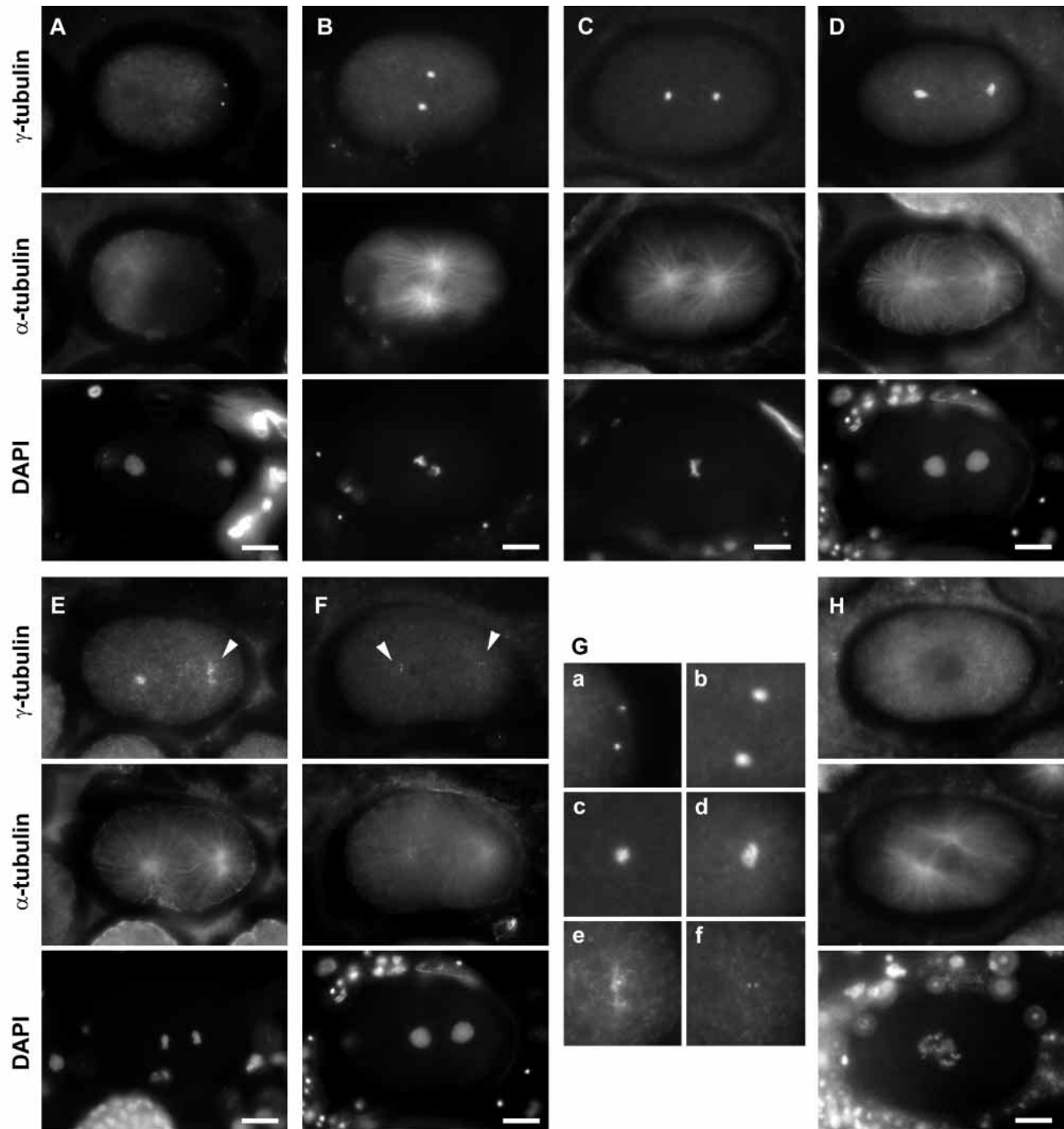


**Fig. 4.** Distribution of  $\gamma$ -tubulin during the first mitotic division of the *C. elegans* embryo. (A-H) Immunostaining of wild-type embryos with affinity-purified anti- $\gamma$ -tubulin antibody (upper panels), anti- $\alpha$ -tubulin antibody (middle panels) and DAPI (lower panels) is shown. Anterior is towards the left. (A)  $\gamma$ -Tubulin is detected at the two duplicated centrosomes adjacent to the sperm pronucleus. An increasing amount of  $\gamma$ -tubulin could be visualized at the centrosomes from prophase to anaphase (B-D), concomitantly with an increase in microtubule nucleation. At telophase (E)  $\gamma$ -tubulin staining is reduced, and the centrosome of the P<sub>1</sub> blastomere (right blastomere) displays a characteristic flattening (arrowhead). During the next interphase (F)  $\gamma$ -tubulin staining is restricted to the centriole pair at each centrosome (arrowheads). A few microtubules are nucleated. (G) A twofold enlargement of the  $\gamma$ -tubulin staining from the previous panels, the small letters refer to the panel labeled by the corresponding capital letter. (H) Incubation of the anti- $\gamma$ -tubulin antibody with the peptide, the small letters refer to the panel labeled by the corresponding capital letter. (H) Incubation of the anti- $\gamma$ -tubulin antibody with the peptide used for immunization abolishes the staining. Scale bars: 10  $\mu$ m in A-F,H.

detect a diffuse cytoplasmic  $\gamma$ -tubulin staining and no centrosomes (Fig. 3B). Immunostaining of mature oocytes failed to reveal any  $\gamma$ -tubulin at the poles of both meiosis I and meiosis II spindles (Fig. 3C and data not shown). These results

are consistent with the acentriolar mode of spindle assembly described for oogenesis in *C. elegans* (Albertson, 1984) and suggest that centrioles are eliminated during the early stages of meiosis.

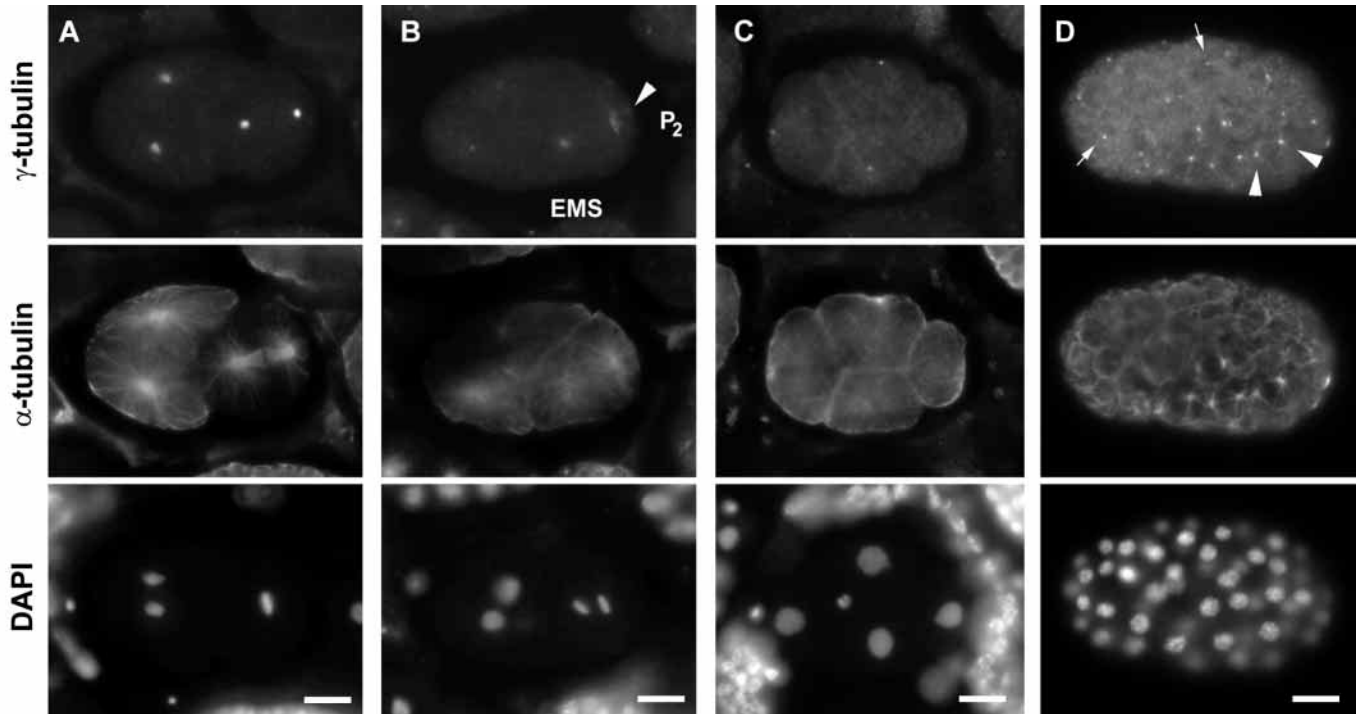


**Fig. 5.**  $\gamma$ -Tubulin localization during the second mitotic division (A–C) and late embryonic stages (D). Immunostaining of wild-type embryos with affinity-purified anti- $\gamma$ -tubulin antibody (upper panels), anti- $\alpha$ -tubulin antibody (middle panels) and DAPI (lower panels) is shown. (A) Division in the P<sub>1</sub> blastomere (on the right) is slightly delayed in regard to the AB blastomere. The transition from a compact organization of the  $\gamma$ -tubulin signal (P<sub>1</sub> blastomere in metaphase) to a decondensed form (AB blastomere in anaphase) can easily be visualized. (B) In anaphase, the centrosome of the future P<sub>2</sub> blastomere flattens (arrowhead). (C) Four-cell stage embryos in interphase present a poorly organized microtubule cytoskeleton and a  $\gamma$ -tubulin staining restricted to the centrosomes. The centrosome of the P<sub>2</sub> blastomere is out of the focal plane. (D) During late embryonic stages (here an embryo containing about 100 nuclei),  $\gamma$ -tubulin staining is detected at both interphase (arrows) and mitotic centrosomes (arrowheads). Recruitment of  $\gamma$ -tubulin in mitosis is moderate by comparison with early embryonic stages. Scale bars: 10  $\mu$ m.

To analyze the localization of  $\gamma$ -tubulin during spermatogenesis, we examined the spermatheca of the hermaphrodite gonad and identified spermatocytes undergoing meiotic division.  $\gamma$ -Tubulin staining was detected at the poles of these spindles as focused dots (Fig. 3D) corresponding to the centrosomes. Mature sperm cells were also observed, showing a weak dot staining at the position expected for the centrosomes (Fig. 3E).

#### Distribution of $\gamma$ -tubulin during early embryonic stages

$\gamma$ -Tubulin shows a striking accumulation at the mitotic centrosomes of *C. elegans* embryos followed by a strong reduction of the signal. This pattern is easily visualized during the first division. As the embryo develops, the mitotic accumulation of  $\gamma$ -tubulin is less and less dramatic.

After fertilization,  $\gamma$ -tubulin was localized at the sperm centrosome (Fig. 4A). As the duplicated centrosomes organize the first mitotic spindle,  $\gamma$ -tubulin was detected in increasing amount at the poles concomitantly with the enlargement of the mitotic asters (Fig. 4B,C). During anaphase, the  $\gamma$ -tubulin signal at both centrosomes showed a spindle-like morphology with the orientation of each structure perpendicular to each other, the centrosome of the AB blastomere lying in the anterior-posterior axis of the embryo (Fig. 4D). This deformation of the centrosomes was most easily visualized during the first mitotic division and could be the consequence

of the forces that act on astral microtubules to orient the spindles perpendicular to each other. A scattering and decrease in  $\gamma$ -tubulin staining was observed in telophase with the characteristic flattening of the centrosome of the P<sub>1</sub> blastomere (Fig. 4E, arrowhead). During the subsequent interphase, the  $\gamma$ -tubulin signal was found restricted to – or very near – the centrosomes (Fig. 4F, arrowheads; compare with  $\alpha$ -tubulin staining). Few microtubules emanating from the centrosomes could be observed.

The second mitotic division of the embryo reproduces the stages described above. It should be noted that a flattening of the centrosome that would be inherited by the P<sub>2</sub> blastomere was visualized (Fig. 5B, arrowhead). This morphological change was not observed in the AB blastomere (Fig. 5A). Interphase centrosomes showed a small amount of  $\gamma$ -tubulin and a poorly organized microtubule cytoskeleton (Fig. 5C). In late embryonic stages, centrosomal  $\gamma$ -tubulin was detected in both interphase and mitotic cells (Fig. 5D), but the amount of protein located at the mitotic centrosomes was much less abundant than during the first mitotic divisions.

No  $\gamma$ -tubulin staining was observed on spindle microtubules and midbodies at any stage.

#### Disruption of $\gamma$ -tubulin expression by RNAi

Injection of double-stranded RNA (RNAi) has been reported as a powerful method with which to specifically interfere with gene expression in *C. elegans* (Fire et al., 1998). Soaking the

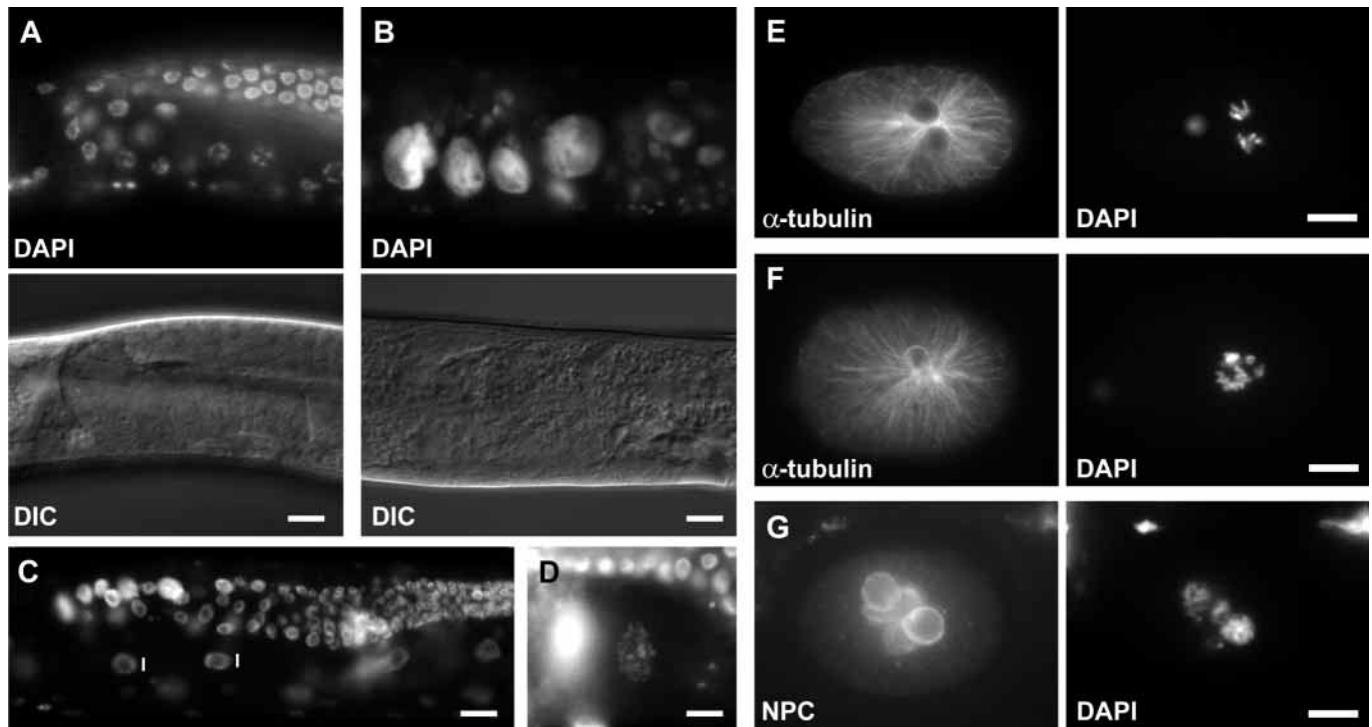


**Fig. 6.** Mitotic cells undergo polyploidization after  $\gamma$ -tubulin double-stranded RNA treatment. (A-D) Adults were fixed and stained with DAPI after soaking in RNA. (A) A control experiment showing a wild-type gonad. (B-D) Phenotypes of  $\gamma$ -tubulin double-stranded RNA soaking experiments. (B) A severe phenotype. The gonad is disrupted and contains only a few highly polyploid nuclei. (C) A mild phenotype, with a progressive polyploidization of germ cells along the gonad. Intestine nuclei are indicated by a vertical line. (D) A polyploid nucleus in diakinesis. Embryos from larvae soaked in  $\gamma$ -tubulin double-stranded RNA were stained with DAPI and antibodies against  $\alpha$ -tubulin (E,F) and nuclear pore complex (NPC) (G). In E, the two pronuclei are separated from each other. The nuclear membrane in (F) has disassembled and the chromosomes display a rosette configuration. (F) is a polyploid embryo. The staining of the nuclear membrane shows that several independent nuclei were formed. Scale bars: 10  $\mu$ m.

worms directly in the RNA solution also appears to be efficient for several genes (Timmons and Fire, 1998). We thus took advantage of this protocol to study the requirements in  $\gamma$ -tubulin at different stages of the worm life-cycle. We first analyzed the effect of RNA soaking on young larvae and embryos (which will hatch in the RNA solution). The animals were allowed to recover after soaking and young adults were transferred to individual plates. Under these conditions, soaking in  $\gamma$ -tubulin double-stranded RNA resulted in 93% adult sterility (assessed 3 days after transfer;  $n=60$ ). Soaked worms showed highly disorganized gonadal tissues and did not lay any eggs.

To characterize the defects leading to sterility further, worms were fixed and stained with DAPI (Fig. 6). Microscopy analysis revealed extremely polyploid nuclei in the gonad of hermaphrodites. For the most severe phenotype observed, the gonad was strongly disrupted, containing a few cells with giant nuclei (Fig. 6B). Mild phenotypes showed a progressive polyploidization of germ cells from distal to proximal in the gonad (Fig. 6C). In this case, the shape of the gonad appeared normal. Interestingly, diakinesis stages could be observed at the proximal side of the gonad (Fig. 6D), suggesting that polyploid cells were able to undergo meiosis. However, these oocytes did not develop any further, and accumulated into the gonad. These results suggest that mitotic germ cells undergo multiple cycles of DNA replication without completing

cytokinesis, consistent with a defect in mitotic spindle assembly. These polyploid cells are still able to respond to the signals triggering their entry in meiosis, depending on their position inside the gonad. The other tissues were not affected by double-stranded RNA.

To analyze the role of  $\gamma$ -tubulin for embryonic progression, animals were synchronized and L3-L4 larvae were soaked as before. Under these conditions mitotic germ cells were not affected in adult hermaphrodites, which would lay numerous embryos. Gravid adults were methanol fixed, the embryos stained with DAPI, and antibodies specific to  $\alpha$ - and  $\gamma$ -tubulins were appeared. The vast majority of embryos contained a nucleus showing various degrees of polyploidization. We observed embryos that were either in interphase or mitosis, suggesting that their DNA content increased through multiple rounds of DNA synthesis in the absence of chromosome segregation.

All stages of meiosis were observed in newly fertilized embryos. A careful analysis of the number of polar bodies failed to demonstrate any difference between RNAi-treated and control embryos. In both cases, the two polar bodies could be visualized in more than 90% ( $n>100$ ) of the embryos, suggesting that embryos lacking  $\gamma$ -tubulin are still able to proceed through meiosis. After migrating, the two pronuclei were not found juxtaposed as in wild-type embryos, but remained separated from each other (Fig. 6E). Microtubules

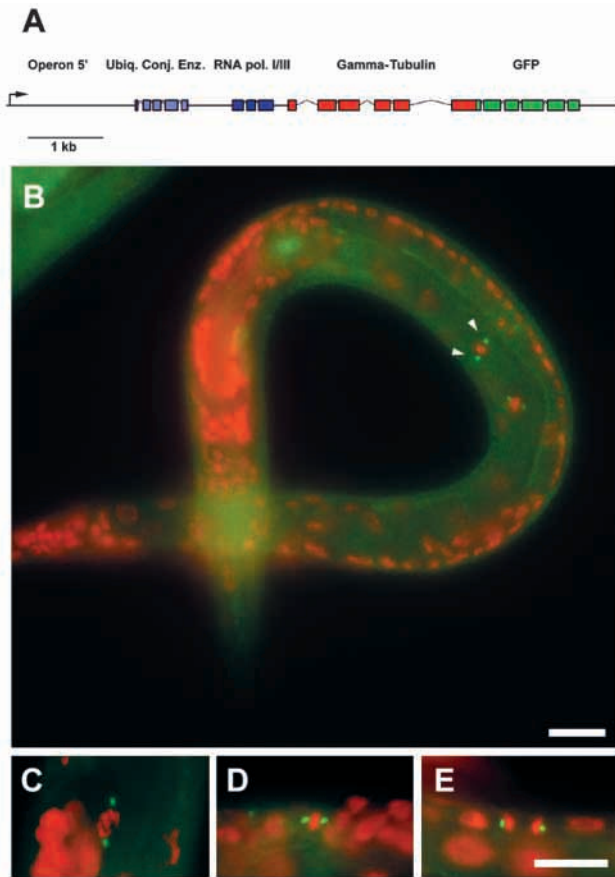


**Fig. 7.**  $\gamma$ -Tubulin::GFP is localized at mitotic centrosomes. (A) Gene structure of the  $\gamma$ -tubulin operon as determined by the *C. elegans* sequencing consortium.  $\gamma$ -Tubulin is the third and last gene of the operon. The  $\gamma$ -tubulin::GFP construct includes all upstream regulatory sequences and the two other genes of the operon. The GFP sequence was fused in frame with the 3' end of the  $\gamma$ -tubulin coding sequence. (B-E) Expression of  $\gamma$ -tubulin::GFP fusion gene in larvae. GFP is detected in green and the image merged with the DAPI staining (red). (B)  $\gamma$ -Tubulin::GFP is detected in all cells as a diffuse staining and concentrated at the mitotic centrosomes of the dividing cells of the forming vulva (arrows). (C-E) Mitotic figures detected during larval development: prophase (C), metaphase (D) and telophase (E). Scale bars: 10  $\mu$ m.

were organized as a monopolar aster centered between the two pronuclei. After nuclear envelope disassembly chromosomes displayed a rosette configuration, typical for monopolar spindles (Fig. 6F). 74% ( $n=38$ ) of young embryos in metaphase I showed chromosomes located in the posterior half of the embryo. The nuclei of older (polyploid) embryos were most often found in the middle of the embryo (70%;  $n=47$ ), suggesting that the chromatin mass will relocate to the center of the embryo after a mitotic cycle. Immunofluorescent staining of the nuclear membrane of interphase polyploid embryos revealed multiple nuclei in all embryos observed ( $n>100$ ; Fig. 6G). No  $\gamma$ -tubulin staining was detected in these embryos (data not shown).

Taken together, these results suggest that meiosis is completed in the absence of  $\gamma$ -tubulin and that the female pronucleus is still capable of migrating towards the posterior male pronucleus. However the presence of multiple

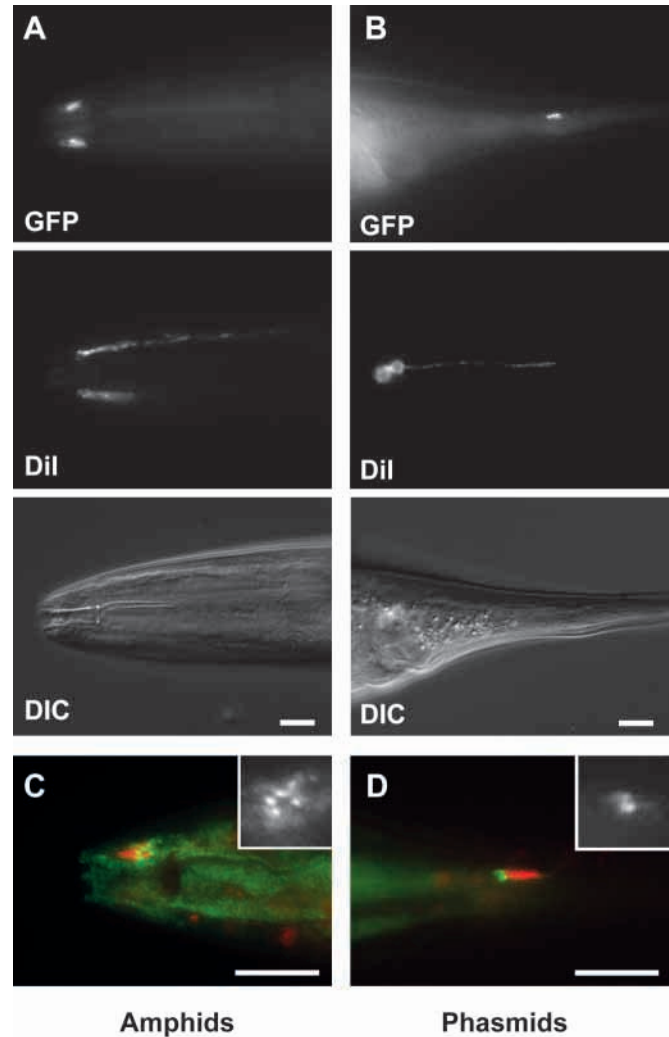


**Fig. 8.** Accumulation of  $\gamma$ -tubulin::GFP at basal bodies. Amphid (A) and phasmid (B) neuronal processes were detected in transgenic worms by filling with the fluorescent dye DiI. In both cases, GFP fluorescence was detected at the openings of the dendrites. (C,D) Cilia were stained by immunofluorescence with GT335 antibody (red) and the image merged with GFP signal (green). GFP is localized at the base of both amphid (C) and phasmid (D) cilia. Inserts show twofold magnifications of the GFP signal; individual basal bodies can be resolved. The second amphid or phasmid in (B-D) is out of the focal plane. Scale bars: 10  $\mu$ m.

independent nuclei at later stages suggests that pronuclear fusion is impaired in  $\gamma$ -tubulin-depleted embryos.

Control experiments included soaking of young larvae in mitogen-activated protein kinase (*mpk-1*) double-stranded RNA. 52% of the animals showed a reduced fertility (less than 50 progenies, assessed 3 days after recovery;  $n=50$ ), including a complete sterility for 62% of the affected adults. Staining of the nuclei by DAPI revealed meiotic cells unable to progress from pachytene to diakinesis in the gonad (not shown), consistent with the phenotype reported for the *mpk-1* mutant (Church et al., 1995). By contrast, 100% of the larvae soaked in medium gave fertile adults ( $n=40$ ). Embryos from these animals were used as a control to follow the early events of embryogenesis.

### $\gamma$ -Tubulin::GFP is localized at the mitotic centrosomes in post-embryonic dividing cells

To determine the distribution of  $\gamma$ -tubulin in postembryonic cells, we generated a reporter gene construct containing the genomic sequence of the  $\gamma$ -tubulin gene fused in-frame to GFP. As the  $\gamma$ -tubulin gene is part of an operon, we included the sequences corresponding to the two other genes of the operon, as well as the common regulatory sequences (Fig. 7A). The transgenic animals obtained started to express the construct during late embryogenesis. In larvae, all tissues (with the exception of the gonad, where transgenes are silenced in *C. elegans*) presented a faint and diffuse staining. This result is consistent with previous reports showing that most  $\gamma$ -tubulin is distributed in the cytoplasm as a soluble pool in the cell (Moudjou et al., 1996; Oegema et al., 1999; Khodjakov and Rieder, 1999). However, we were also expecting to detect  $\gamma$ -tubulin accumulated at the centrosomes of all cells. A careful analysis of larval stages showed that a strong GFP fluorescence could be detected at the mitotic centrosomes of hypodermal and vulval cells undergoing mitosis (Fig. 7B) but no centrosomal staining was visible in these cells in interphase. Thus, we believe that our  $\gamma$ -tubulin::GFP construct is functional, and that interphase centrosomes do not contain enough  $\gamma$ -tubulin to allow its detection. Centrosome-associated  $\gamma$ -tubulin was detected from prophase to telophase in postembryonic mitotic cells (Fig. 7C-E). Again, no signal was detected on spindle microtubules and at midbodies.

### $\gamma$ -Tubulin::GFP accumulates at the basal bodies of amphid and phasmid sensory neurons

We next investigated whether non-centrosomal  $\gamma$ -tubulin::GFP structures could be identified in transgenic animals. In adults, a striking distribution of GFP was visualized as two symmetrically distributed patches in the tip of the head and two pairs of dots in the tail (Fig. 8A,B). This expression pattern suggests that  $\gamma$ -tubulin::GFP could be localized at the opening of amphid and phasmid neurons. Amphids are a pair of lateral organs located at the tip of the head. Each amphid is composed of 12 cilia emanating from 12 sensory neurons. The pair of lateral phasmids are located in the tail of the animal. Each phasmid comprises two cilia. These cilia are non-motile and act as the main chemosensory organs of the worm (Perkins et al., 1986).

The dendrites corresponding to amphid and phasmid neurons were stained by dye-filling of living transgenic animal. As shown in Fig. 8, the GFP localization was coincident with the opening of these neurons. To confirm this localization, cilia were stained by immunofluorescence with GT335, a monoclonal antibody that recognizes axonemal tubulin from many species (Bobinnec et al., 1999; Million et al., 1999).  $\gamma$ -Tubulin::GFP was detected at the base of both amphid and phasmid cilia (Fig. 8C,D). Several dots were visualized for each amphid and a pair of dot for each phasmid. To a lesser extent, some signal was seen around the basal bodies and along the cilia. These data suggest that  $\gamma$ -tubulin is present at all basal bodies of phasmid and amphid cilia and possibly in basal body-associated structures.

### A lattice of $\gamma$ -tubulin::GFP distributes at the apical membrane of intestinal cells

In addition to basal bodies, a continuous line of GFP fluorescence is detected at the apical side of intestinal cells in

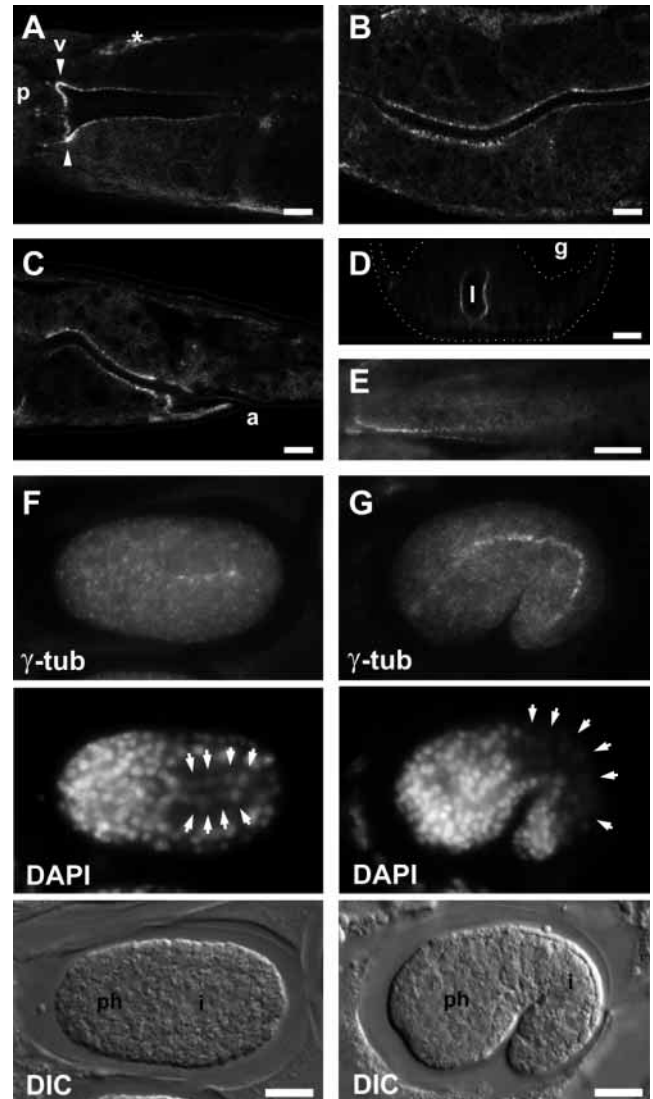


**Fig. 9.** Non-centrosomal  $\gamma$ -tubulin is distributed at the apical side of intestine cells. (A-D) Adult transgenic worms were methanol-fixed and localization of GFP examined by confocal microscopy. Anterior (A), middle (B) and posterior (C) segments of the intestine show a continuous lattice of  $\gamma$ -tubulin::GFP at the apical side of intestinal cells. The labeling includes the pharyngeal-intestinal valve cells (v, arrowheads) between the pharynx (p) and the intestine and extends all along the intestine up to the anus (a). The signal indicated by a star is not specific of the reporter gene. (D) Z-section through the intestine, showing distribution of GFP throughout the apical membranes. The body wall and the localization of the gonad (g) are underlined with white dots. The lumen (l) of the intestine is indicated. (E) Surface of the apical membrane in the anterior segment of the intestine viewed by conventional epifluorescence microscopy; small dots composing the lattice of  $\gamma$ -tubulin::GFP are resolved. (F,G) Immunofluorescence analysis of late embryonic stages with anti- $\gamma$ -tubulin antibody. A lattice of  $\gamma$ -tubulin is first detected in intestinal cells of embryos 280 minutes after the first cleavage (F). Note the apical positioning of the intestinal nuclei, indicating that these cells are polarized. The  $\gamma$ -tubulin signal extends and intensifies concomitantly with the development of the intestine. (G) shows an embryo 400 minutes after the first cleavage. Arrows point to intestinal nuclei. Localization of the pharynx (ph) and intestine (i) are shown on the corresponding Nomarski (DIC) images. Scale bars: 10  $\mu$ m.

transgenic adults. Confocal sections through the middle of the intestinal tract show a compact apical localization of  $\gamma$ -tubulin::GFP from the pharyngeal-intestinal valve cells to the rectum (Fig. 9A-C). It is interesting to note that both intestinal and valve cells, as well as some rectal cells, are polarized cells with microvilli on their apical surface (White, 1988). These data are consistent with a role of  $\gamma$ -tubulin in the polarization of the microtubular network in these cells. Transverse sectioning of the animals through the Z dimension by confocal microscopy demonstrates a uniform distribution of the GFP throughout the apical membrane of intestine cells (Fig. 9D). This signal was further analyzed by conventional epifluorescence microscopy in order to obtain a better resolution of the  $\gamma$ -tubulin::GFP structures. Focusing on the surface of the larger anterior intestine tract, we could detect small dots of GFP, smaller than centrosomes, regularly spaced out (Fig. 9E). A diffuse GFP signal was also observed in the cytoplasm of intestine cells, but no foci that might correspond to centrosomal  $\gamma$ -tubulin could be identified.

We next investigated, using immunofluorescence, whether  $\gamma$ -tubulin could be detected in intestinal cells during embryogenesis. A positive signal appeared in embryos 280 minutes after the first cleavage as a line of  $\gamma$ -tubulin between intestinal precursor cells (Fig. 9F). As the embryos developed, the  $\gamma$ -tubulin signal extended and intensified (Fig. 9G). This distribution is likely to reflect the occurrence of polarization in these cells, as suggested by the apical localization of the nuclei, followed by a relocalization of  $\gamma$ -tubulin at the apical membrane.

Distribution of  $\gamma$ -tubulin in wild-type adults was also analyzed by immunofluorescence microscopy with the anti- $\gamma$ -tubulin antibody. Localization of the protein was confirmed at basal bodies of amphid and phasmid neurons and at the apical membrane of intestine cells. Centrosomal foci were not detected in any tissues (not shown).

## DISCUSSION

### The $\gamma$ -tubulin of *C. elegans*

The complete sequence of the genome of *C. elegans* reveals a complex multigenic tubulin family that comprises 16 members. By comparison, four tubulin genes are found in the *S. cerevisiae* genome, 11 in the *Drosophila* genome and 13 have been characterized so far in mouse. The reasons for such a complexity should certainly be questioned, and *C. elegans*, because of the availability of the genome sequence and the easy observation of differentiated tissues, is certainly one of the most suitable organism for this purpose. One could envision a detailed analysis of the expression pattern and subcellular localization for each of these tubulins. Such a study could produce important data about the requirements of specialized tubulin isotypes for differentiation.

The 16 *C. elegans* genes distribute as nine  $\alpha$ -, six  $\beta$ - and one  $\gamma$ -tubulin isotype. No sequences related to  $\delta$ - and  $\epsilon$ -tubulins (Dutcher and Trabuco, 1998; Chang and Stearns, 2000) could be identified. There is still a possibility that these singular tubulins, being not under an evolutionary pressure that is as strong as for the  $\alpha/\beta$ s, would be present in the *C. elegans* genome but difficult to characterize. Additional sequences from other organisms will be necessary to define the conserved domains in these sequences.

The  $\gamma$ -tubulin sequences from various organisms show some discrepancy as well. The *S. cerevisiae*  $\gamma$ -tubulin TUB4 in particular shows only 40% identity with the other members. We show here that like *S. cerevisiae* TUB4, the *C. elegans*  $\gamma$ -tubulin gene is quite divergent from all other  $\gamma$ -tubulins. This has made the identification of this gene rather difficult by means of sequence comparison, leading to a controversial discussion about whether this sequence belongs to the  $\gamma$ -tubulin family or whether it should define a new class of tubulins (Burns, 1995; Burns and Farrell, 1996; Keeling and Logsdon, 1996). Our data clearly demonstrate that, although divergent, this gene encodes a genuine  $\gamma$ -tubulin.

### $\gamma$ -Tubulin during meiosis and mitosis

The  $\gamma$ -tubulin gene of *C. elegans* is a ubiquitous, maternal gene. In the hermaphrodite gonad, the protein was detected at the centrosomes of mitotic germ cells and all along male meiosis. Only a small amount of protein is present at sperm centrioles, which is expected from a peculiar centrosome that does not act as a microtubule-organizing center. During female meiosis, centrosomes are not detectable anymore in oocytes arrested in prophase of the first meiotic division, and meiotic I and II spindles do not contain any detectable amount of  $\gamma$ -tubulin. Whereas most species show a  $\gamma$ -tubulin staining at the meiotic spindle poles, an absence of staining has also been described for *Drosophila*. In this organism, the requirements in  $\gamma$ -tubulin for meiosis are controversial (Tavosanis et al., 1997; Wilson and Borisy, 1998). Our results from RNAi experiments suggest a lack of function for *C. elegans*  $\gamma$ -tubulin during meiosis. One essential difference in the meiotic pathway is the absence of centrioles, which should lead to the scattering of the centrosomal proteins and microtubule nucleation machinery. In *C. elegans*, this hypothesis is supported by the distribution of ZYG-9, a factor essential for microtubule organization. The protein is detected around the centrosomes during mitotic divisions but appears scattered throughout the metaphase spindle during meiosis (Matthews et al., 1998). Some additional factors would be necessary to overcome the absence of a focused centrosome. MEI-1, a meiotic-spindle specific component that needs to be inactivated for mitosis to proceed (Clark-Maguire and Mains, 1994; Srayko et al., 2000) is a good candidate for this function.

$\gamma$ -Tubulin is recruited around sperm centrioles after fertilization, and accumulates massively at the centrosome during prophase of the first embryonic division. The centrosome undergoes striking morphological changes from metaphase to interphase. The compact structure visualized in metaphase changes into a spindle-like shape in anaphase before losing most of the  $\gamma$ -tubulin in telophase. In interphase, the  $\gamma$ -tubulin signal is similar in size to that of  $\alpha$ -tubulin, suggesting that most of the  $\gamma$ -tubulin protein left resides inside – or very near – the centriole. Concomitantly with these events, the number of microtubules nucleated at the centrosomes decreases considerably from telophase. This ‘catastrophic’ disassembly of  $\gamma$ -tubulin from the centrosome as cells exit mitosis has been reported in mammalian cells, and is likely to be due to the release of most of the pericentriolar material into the cytoplasm (Dictenberg et al., 1998). In *C. elegans*, this transition in the centrosomal matrix state can be easily visualized, probably because of the huge size of the

centrosomes in the one-cell stage embryo. In addition, partly disrupted pericentriolar material could be more sensitive to the tension exerted by spindle microtubules. This would explain the morphological changes of the centrosome into a spindle-like shape and also its flattening. Indeed, as pointed out by Keating and White (1998), the centrosome located near the cortical site responsible for P granule segregation (Strome and Wood, 1983) and reorientation of the spindle in the P<sub>1</sub> blastomere (Hyman and White, 1987; Hyman, 1989) undergoes a spectacular flattening during anatelephase. We show here that this flattening also occurs in the P<sub>2</sub> blastomere, suggesting that this cortical site could be responsible for the deformation of its attached centrosome. It has not been possible to determine whether this event is recurrent during the subsequent divisions of the P lineage, because of the small size of the centrosomes and the cells.

In the absence of  $\gamma$ -tubulin, we show that completion of meiosis still occurs. Migration of the female pronucleus is not impaired either. We cannot rule out the possibility that a small fraction of the  $\gamma$ -tubulin pool was left intact after RNAi. These molecules could be sufficient to allow the assembly of microtubules that would self-organize into a monopolar spindle. These microtubules would, in turn, be able to capture the female pronucleus. However, pronuclear fusion does not occur. In wild-type embryos the centrosomes are positioned in front of each other at the time of pronuclear juxtaposition, each one connected to both pronuclei. Such a configuration is impossible in the absence of any centrosome in  $\gamma$ -tubulin-depleted embryos, which probably explains the failure of pronuclear fusion.

### Distribution of $\gamma$ -tubulin in adult tissues

About 5 hours after the first cleavage, most cell proliferation is completed, and cell differentiation begins. From this stage, centrosomes are difficult to visualize by immunofluorescence microscopy. A few postembryonic divisions will take place during the larval stages, most of them in hypodermal, intestine and vulval cells. The use of a GFP reporter gene allowed us to detect  $\gamma$ -tubulin at the mitotic centrosomes of these cells, but no centrosomal localization was observed in these same tissues during interphase. Later in adults, centrosomes cannot be detected in any tissue other than mitotic germ cells and male meiotic cells. The simplest interpretation for this observation is that the amount of  $\gamma$ -tubulin at interphase centrosomes is below the level of detection of a conventional epifluorescence microscope.

Alternatively, centrosomes could be inactivated or even discarded in differentiated cells. A centrosome is defined as a pair of centrioles surrounded by a pericentriolar matrix. As the centrioles are responsible for the cohesion of the centrosome itself (Bobinnec et al., 1998), a loss of the centrosome implies a loss of the centrioles. Such a situation has been observed during female meiosis and for wing epidermal cells in *Drosophila* (Mogensen and Tucker, 1987) and has been suggested to occur during myogenesis in vitro (Tassin et al., 1985). An important question raised by these data how microtubule nucleation takes place in these cells. In mammalian cells, removal of the whole centrosome does not impair cell function in interphase, but blocks cell division (Maniotis and Schliwa, 1991). Interphase microtubules may thus self-organize in the absence of centrosomes without any

consequence for cell viability, and presumably be nucleated from cytoplasmic factors (Vorobjev et al., 1997). In adult *C. elegans*, it should be noted that most cytoplasmic microtubules are composed of 11 protofilaments. Some 15-protofilament microtubules, based on the  $\beta$ -tubulin isotype MEC-7, are found in a set of mechanosensory neurons (Chalfie and Thomson, 1982; Savage et al., 1989). The cilia are the only structure described to contain 13-protofilament microtubules at the A subfiber of the outer doublets (Chalfie and Thomson, 1982). As 13-protofilaments microtubules are characteristic of centrosome-nucleated microtubules (Evans et al., 1985), one can envision that most of the microtubules in *C. elegans* adult tissues are nucleated through a non-centrosomal pathway, involving, or not,  $\gamma$ -tubulin complexes scattered into the cytoplasm. These cytoplasmic microtubule-nucleating complexes may not be associated with the regulatory factors found at the centrosome. This hypothesis could be ideally tested using microtubule-regrowth assays. As an alternative, the characterization of other centrosomal components and their subcellular localization would help to clarify the mechanisms of microtubule nucleation and organization in differentiated cells.

Our data suggest that the centrosome is an organelle dedicated to mitosis, and that a profound reorganization of the microtubule-organizing material takes place in differentiated tissues, in relation to the function of the cell. The adaptation of microtubule nucleation to differentiated cells could involve the use of some specific  $\alpha/\beta$ -tubulin isotypes and/or microtubule-stabilization factors in order to obtain a less dynamic population of microtubules. A close investigation of these mechanisms is essential to achieve a complete understanding of the microtubule cytoskeleton regulation and function.

We thank Yuji Kohara for the cDNAs, Alan Coulson for the cosmid F58A4, Andrew Fire for the expression vector pPD95-75, Bernard Eddé for the kind gift of GT335 antibody, and Makoto Adachi for help in cDNA cloning and 5' RACE experiments. We are grateful to all the instructors of the *C. elegans* courses at the Cold Spring Harbor Laboratory for their excellent teaching. We also thank Dr Alain Debec for stimulating discussions and comments during the course of this study. This work was supported by grants-in-aid from the Ministry of Education, Science and Culture of Japan to E.N. Y.B. was supported by a Lavoisier fellowship from the Ministère des Affaires Étrangères (France).

### REFERENCES

- Albertson, D. G. (1984). Formation of the first cleavage spindle in nematode embryos. *Dev. Biol.* **101**, 61-72.
- Bobinnec, Y., Khodjakov, A., Mir, L. M., Rieder, C. L., Eddé, B. and Bornens, M. (1998). Centriole disassembly in vivo and its effect on centrosome structure and function in vertebrate cells. *J. Cell Biol.* **143**, 1575-1589.
- Bobinnec, Y., Marcaillou, C. and Debec, A. (1999). Microtubule polyglutamylated in *Drosophila melanogaster* brain and testis. *Eur. J. Cell Biol.* **78**, 671-674.
- Brenner, S. (1974). The genetics of *Caenorhabditis elegans*. *Genetics* **77**, 71-94.
- Burns, R. G. (1995). Identification of two new members of the tubulin family. *Cell Motil. Cytoskeleton* **31**, 255-258.
- Burns, R. G. and Farrell, K. W. (1996). Getting to the heart of  $\beta$ -tubulin. *Trends Cell Biol.* **6**, 297-303.
- C. elegans* Sequencing Consortium (1998). Genome sequencing of the

- nematode *C. elegans*: a platform for investigating biology. *Science* **282**, 2012-2018.
- Carazo-Salas, R. E., Guarguaglini, G., Gruss, O. J., Segref, A., Karsenti, E. and Mattaj, I. W.** (1999). Generation of GTP-bound Ran by RCC1 is required for chromatin-induced mitotic spindle formation. *Nature* **400**, 178-181.
- Cassata, G., Kagoshima, H., Prétôt, R. F., Aspöck, G., Niklaus, G. and Bürglin, T. R.** (1998). Rapid expression screening of *Caenorhabditis elegans* homeobox open reading frames using a two-step polymerase chain reaction promoter-GFP reporter construction technique. *Gene* **212**, 127-135.
- Chalfie, M. and Thomson, J. N.** (1982). Structural and functional diversity in the neuronal microtubules of *Caenorhabditis elegans*. *J. Cell Biol.* **93**, 15-23.
- Chang, P. and Stearns, T.** (2000).  $\delta$ -tubulin and  $\epsilon$ -tubulin: two new human centrosomal tubulins reveal new aspects of centrosome structure and function. *Nat. Cell Biol.* **2**, 30-35.
- Church, D. L., Guanand, K. and Lambie, E. J.** (1995). Three genes of the MAP kinase cascade, *mek-2*, *mpk-1/sur-1* and *let-60 ras*, are required for meiotic cell cycle progression in *Caenorhabditis elegans*. *Development* **121**, 2525-2535.
- Clark-Maguire, S. and Mains, P. E.** (1994). Localization of the *mei-1* gene product of *Caenorhabditis elegans*, a meiotic-specific spindle component. *J. Cell Biol.* **126**, 199-209.
- Debec, A., Szollozi, A. and Szollozi, D.** (1982). A *Drosophila melanogaster* cell line lacking centrioles. *Biol. Cell* **44**, 133-138.
- Dictenberg, J. B., Zimmerman, W., Sparks, C. A., Young, A., Vidair, C., Zheng, Y., Carrington, W., Fay, F. S. and Doxsey, S. J.** (1998). Pericentriar and gamma-tubulin form a protein complex and are organized into a novel lattice at the centrosome. *J. Cell Biol.* **141**, 163-174.
- Dutcher, S. K. and Traub, E. C.** (1998). The *UNI3* gene is required for assembly of basal bodies of *Chlamydomonas* and encodes  $\delta$ -tubulin, a new member of the tubulin superfamily. *Mol Biol. Cell* **9**, 1293-1308.
- Evans, L., Mitchison, T. and Kirschner, M.** (1985). Influence of the centrosome on the structure of nucleated microtubules. *J. Cell Biol.* **100**, 1185-1191.
- Fire, A., Xu, S., Montgomery, M. K., Kostas, S. A., Driver, S. E. and Mello, C. C.** (1998). Potent and specific genetic interference by double-stranded RNA in *Caenorhabditis elegans*. *Nature* **391**, 806-811.
- Fuller, S. D., Gowen, B. E., Reinsch, S., Sawyer, A., Buendia, B., Wepf, R. and Karsenti, E.** (1995). The core of the mammalian centriole contains  $\gamma$ -tubulin. *Curr. Biol.* **5**, 1384-1393.
- Harlow, E. and Lane, D.** (1988). *Antibodies, A Laboratory Manual*. New York: Cold Spring Harbor Laboratory Press.
- Heald, R., Tournebise, R., Habermann, A., Karsenti, E. and Hyman, A.** (1997). Spindle assembly in *Xenopus* egg extracts: respective roles of centrosomes and microtubule self-organization. *J. Cell Biol.* **138**, 615-628.
- Hedgecock, E. M., Culotti, J. G., Thomson, J. N. and Perkins, L. A.** (1985). Axonal guidance mutants of *Caenorhabditis elegans* identified by filling sensory neurons with fluorescein dyes. *Dev. Biol.* **111**, 158-170.
- Hyman, A. A. and White, J. G.** (1987). Determination of cell division axes in the early embryogenesis of *Caenorhabditis elegans*. *J. Cell Biol.* **105**, 2123-2135.
- Hyman, A. A.** (1989). Centrosome movement in the early divisions of *Caenorhabditis elegans*: a cortical site determining centrosome position. *J. Cell Biol.* **109**, 1185-1193.
- Joshi, H. C., Palacios, M. J., McNamara, L. and Cleveland, D. W.** (1992). Gamma-tubulin is a centrosomal protein required for cell cycle dependent microtubule nucleation. *Nature* **356**, 80-83.
- Keating, H. H. and White, J. G.** (1998). Centrosome dynamics in early embryos of *Caenorhabditis elegans*. *J. Cell Science* **111**, 3027-3033.
- Keating, T. K. and Borisy, G.** (1999). Centrosomal and non-centrosomal microtubules. *Biol. Cell* **91**, 321-329.
- Keeling, P. J. and Logsdon, J. M.** (1996). Highly divergent *Caenorhabditis* and *Saccharomyces* tubulins evolved recently from genes encoding  $\gamma$ -tubulin. *Trends Cell Biol.* **6**, 375.
- Khodjakov, A. and Rieder, C. L.** (1999). The sudden recruitment of  $\gamma$ -tubulin to the centrosome at the onset of mitosis and its dynamic exchange throughout the cell cycle, do not require microtubules. *J. Cell Biol.* **146**, 585-596.
- Laemmli, U. K.** (1970). Cleavage of structural proteins during the assembly of the head of bacteriophage T4. *Nature* **227**, 680-685.
- Lewis, J. A. and Flemming, J. T.** (1995). Basic culture methods. In *Caenorhabditis elegans, Modern Biological Analysis of an Organism*. Vol. 48 (ed. H. F. Epstein and D. C. Shakes), pp. 3-28. San Diego: Academic Press.
- Maniotis, A. and Schliwa, M.** (1991). Microsurgical removal of centrosomes blocks cell reproduction and centriole generation in BSC-1 cells. *Cell* **67**, 495-504.
- Matthews, L. R., Carter, P., Thierry-Mieg, D. and Kempheus, K.** (1998). ZYG-9, A *Caenorhabditis elegans* protein required for microtubule organization and function, is a component of meiotic and mitotic spindle poles. *J. Cell Biol.* **141**, 1159-1168.
- Meads, T. and Schroer, T. A.** (1995). Polarity and nucleation of microtubules in polarized epithelial cells. *Cell Motil. Cytoskeleton* **32**, 273-288.
- Mello, C. and Fire, A.** (1995). DNA transformation. In *Caenorhabditis elegans, Modern Biological Analysis of an Organism*. Vol. 48 (ed. H. F. Epstein and D. C. Shakes), pp. 451-482. San Diego: Academic Press.
- Million, K., Larcher, J., Laoukili, J., Bourguignon, D., Marano, F. and Tournier, F.** (1999). Polyglutamylation and polyglycylation of  $\alpha$ - and  $\beta$ -tubulins during in vitro ciliated cell differentiation of human respiratory epithelial cells. *J. Cell Science* **112**, 4357-4366.
- Mogensen, M. M. and Tucker, J. B.** (1987). Evidence for microtubule nucleation at plasma membrane-associated sites in *Drosophila*. *J. Cell Science* **88**, 95-107.
- Mogensen, M.** (1999). Microtubule release and capture in epithelial cells. *Biol. Cell* **91**, 331-341.
- Moritz, M., Braunfeld, M. B., Sedat, J. W., Alberts, B. and Agard, D. A.** (1995). Microtubule nucleation by gamma-tubulin-containing rings in the centrosome. *Nature* **378**, 638-640.
- Moudjou, M., Bordes, N., Paintrand, M. and Bornens, M.** (1996). Gamma-tubulin in mammalian cells: the centrosomal and the cytosolic forms. *J. Cell Sci.* **109**, 875-887.
- Oakley, B. R., Oakley, C. E., Yoon, Y. and Jung, M. K.** (1990). Gamma-tubulin is a component of the spindle pole body that is essential for microtubule function in *Aspergillus nidulans*. *Cell* **61**, 1289-1301.
- Oegema, K., Wiese, C., Martin, O. C., Milligan, R. A., Iwamatsu, A., Mitchison, T. J. and Zheng, Y.** (1999). Characterization of two related *Drosophila* gamma-tubulin complexes that differ in their ability to nucleate microtubules. *J. Cell Biol.* **144**.
- Perkins, L. A., Hedgecock, E. M., Thomson, J. N. and Culotti, J. G.** (1986). Mutant sensory cilia in the nematode *Caenorhabditis elegans*. *Dev. Biol.* **117**, 456-487.
- Ruiz, F., Beisson, J., Rossier, J. and Dupuis-Williams, P.** (1999). Basal body duplication in *Paramecium* requires  $\gamma$ -tubulin. *Curr. Biol.* **9**, 43-46.
- Salas, P. J. I.** (1999). Insoluble  $\gamma$ -tubulin-containing structures are anchored to the apical network of intermediate filaments in polarized CACO-2 epithelial cells. *J. Cell Biol.* **146**, 645-657.
- Savage, C., Hamelin, M., Culotti, J. G., Coulson, A., Albertson, D. G. and Chalfie, M.** (1989). *mec-7* is a beta-tubulin gene required for the production of 15-protofilament microtubules in *Caenorhabditis elegans*. *Genes Dev.* **3**, 870-881.
- Sluder, G., Miller, F. J. and Lewis, K.** (1993). Centrosome inheritance in starfish zygotes. II: Selective suppression of the maternal centrosome during meiosis. *Dev. Biol.* **155**, 58-67.
- Sonnenblick, B. P.** (1950). The early embryology of *Drosophila melanogaster*. In *Biology of Drosophila* (ed. M. Demerec), pp. 62-167. New York: Hafner Publishing.
- Srayko, M., Buster, D. W., Bazirgan, O. A., McNally, F. J. and Mains, P. E.** (2000). MEI-1/MEI-2 katanin-like microtubule severing activity is required for *Caenorhabditis elegans* meiosis. *Genes Dev.* **14**, 1072-1084.
- Starich, T. A., Herman, R. K., Kari, C. K., Yeh, W. H., Schackwitz, W. S., Scuyler, M., Collet, J., Thomas, J. and Riddle, D.** (1995). Mutations affecting chemosensory neurons of *Caenorhabditis elegans*. *Genetics* **139**, 171-188.
- Strome, S. and Wood, W. B.** (1983). Generation of asymmetry and segregation of germline granules in early *C. elegans* embryos. *Cell* **35**, 15-25.
- Sulston, J. and Hodgkin, J.** (1988). Methods. In *The nematode Caenorhabditis elegans* (ed. W. B. Wood), pp. 587-606. Cold Spring Harbor: Cold Spring Harbor Laboratory Press.
- Szöllösi, D., Callarco, P. G. and Donahue, R. P.** (1972). Absence of centrioles in the first and second meiotic spindles mouse oocytes. *J. Cell Sci.* **11**, 521-541.
- Tassin, A. M., Maro, B. and Bornens, M.** (1985). Fate of microtubule-organising centers during myogenesis in vitro. *J. Cell Biol.* **100**, 35-46.
- Tavosanis, G., Llamazares, S., Gouliemos, G. and Gonzalez, C.** (1997).

- Essential role for  $\gamma$ -tubulin in the acentriolar female meiotic spindle of *Drosophila*. *EMBO J.* **16**, 1809-1819.
- Theurkauf, W. E. and Hawley, R. S.** (1992). Meiotic spindle assembly in *Drosophila* females: behavior of nonexchange chromosomes and the effects of mutations in the *nod* Kinesin-like protein. *J. Cell Biol.* **116**, 1167-1180.
- Timmons, L. and Fire, A.** (1998). Specific interference by ingested dsRNA. *Nature* **395**, 854.
- Tucker, J. B., Mogensen, M. M., Paton, C. C., Mackie, J. B. and Henderson, C. G.** (1995). Formation of two microtubule-nucleating sites which perform differently during centrosomal reorganization in a mouse cochlear epithelial cell. *J. Cell Sci.* **108**, 1333-1345.
- Vorobjev, I. A., Svitkina, T. M. and Borisy, G. G.** (1997). Cytoplasmic assembly of microtubules in cultured cells. *J. Cell Sci.* **110**, 2635-2645.
- White, J.** (1988). The anatomy. In *The Nematode Caenorhabditis elegans* (ed. W. B. Wood), pp. 81-122. Cold Spring Harbor: Cold Spring Harbor Laboratory Press.
- Wilson, P. G. and Borisy, G. G.** (1998). Maternally expressed  $\gamma$ Tub37CD in *Drosophila* is differentially required for female meiosis and embryonic mitosis. *Dev. Biol.* **199**, 273-290.
- Zheng, Y., Wong, M. L., Alberts, B. and Mitchison, T.** (1995). Nucleation of microtubule assembly by a  $\gamma$ -tubulin-containing ring complex. *Nature* **378**, 578-583.